A Penalty Finite Element Model for Coupled Heat and Fluid Flows in Continuous Casting of Steel

B. Wiwatanapataphee , Y-H. Wu and P.F. Siew
School of Mathematics and Statistics
Curtin University of Technology
Perth, WA 6001

ABSTRACT

The continuous casting of steel involves the coupled fluid flow - heat transfer phenomenon. Over the past two decades, a great deal of work has been carried out to model the transfer of heat from molten steel to the surrounding mould wall. However, only a few models have been developed to solve coupled turbulent flow and heat transfer with solidification in continuous casting systems. Further studies on modelling the coupled transport problem are still a worthwhile undertaking. In this study a two-dimensional penalty finite element model is developed to study the strongly coupled heat transfer - solidification - turbulent fluid flow in the continuous casting process. The main features of the model are the Navier-Stokes equations for unsteady-state turbulent incompressible viscous fluid flows, the k-ε model of turbulence in the context of eddy viscosity models, and thermal transfer through convection and diffusion. The influence of gap size and thermal contact resistance between the mould wall and the steel strand is taken into account in calculating heat flux from the steel strand surface to the mould cooling-water.

NOMENCLATURE

C morphology constant
C_1, C_2, C_3 positive constants used in (6)
$C_{\varepsilon 1}, C_{\varepsilon 2}$ parameters used in (6)
L latent heat of steel
N number of nodes in an element
R interface thermal contact resistance
S_u, S_T momentum and heat source terms
T temperature of steel
T_L molten temperature of steel
T_S solidified temperature of steel
T_β reference temperature
T_∞ temperature of cooling water
T_{surf} temperature on the strand surface
T_w temperature on the mould wall
T_u temperature of solid flux on its interface with the mould wall
T_{in} pouring temperature of molten steel
T_{ext} external temperature in the spray region of steel casting
U_{cast} casting velocity
U_{in} pouring velocity of molten steel
c_p specific heat of steel
f function defined by (4)
g acceleration due to gravity
gap thickness of lubrication layer
h_∞ mould heat transfer coefficient
h_α steel heat transfer coefficient
k turbulent energy
p pressure in molten steel
t time
u_i fluid velocity component in the *ith* direction
u_r relative velocity defined by u_i-U_{cast}
δ penalty number
ε rate of dissipation of turbulent energy
λ molecular thermal conductivity of steel
λ_{eff} effective thermal conductivity of steel
λ_g thermal conductivity of flux layer
$\sigma_k, \sigma_\varepsilon$ turbulence model constants
σ_t turbulent Prandtl number
σ Stefan-Bolzmann constant
β coefficient of thermal expansion of steel
μ molecular viscosity of steel
μ_{eff} effective viscosity of steel
κ permeability
ρ density of steel
ω emissivity of solid steel

1. INTRODUCTION

The essential features of the continuous casting process are shown in Figure 1. Molten steel is fed from a tundish through a nozzle into a water-cooled mould and solidified steel is continuously extracted from the bottom of the mould at a constant casting speed. During the casting process mould powder is added at the top of the mould and the mould itself oscillates vertically to facilitate the continuous process and to prevent the steel from sticking to the mould walls. The mould powder melts and forms a lubricating layer, referred to as casting flux, in the gap between the solidified steel shell and the mould wall. As the flux moves down the mould wall it solidifies and so a layer of solidified flux forms between the liquid flux and the mould wall. This industrial process involves both fluid flow and heat transfer with solidification. It has been well established that to optimise the casting process, it is essential to understand the mass and heat transfer process occurring in the casting mould. Mathematically, the fluid flow - heat transfer phenomenon is governed by the momentum equations and an energy equation which are strongly coupled through a convective term, a Darcy term and turbulence quantities. Over the last two decades, a number of models have been proposed to study various aspects of the casting process such as heat transfer (Hill et al, 1994, 1997; Wu and Hill, 1994) and the transport of heat and mass (Choudhary and Mazumdar, 1994; Flint, 1990; Shyy et al, 1992). However, only a few studies have solved the coupled turbulent flow and heat transfer with solidification in the continuous casting system. In most studies, the coupled transport problem is solved as a steady state problem and

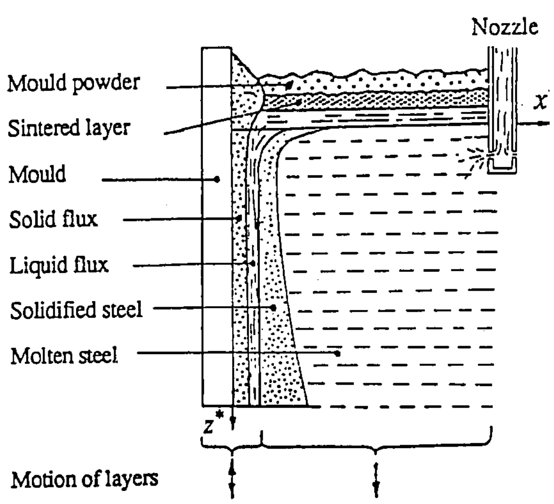

Fig 1. The continuous casting process

commercial codes such as PHOENICS and FIDAP are used for finding the solution. One of the purpose of the present study is to develop an alternative numerical scheme which solves the problem as a strongly coupled transient heat transfer-turbulent flow problem. In contrast to steady state models, the present model does not require a good initial guess of the velocity field in order to achieve convergence of numerical solutions. Another purpose of the present work is to consider the influence of gap size and thermal contact resistance on solidification of steel. In existing models, a parameter representing the average overall heat transfer coefficient between the strand surface and the mould cooling-water is employed, instead of including the lubricating layer, the mould wall and their interface in the computation region. The existing treatment consequently does not permit analysis of some of the important phenomena, such as the effect of mould powder properties, the thickness of lubrication gap and interface thermal contact resistance on the solidification of steel. Thus, the present model is developed to consider the heat transfer across the interface between the lubricating layer and the mould wall. Finally, the developed model is used to determine the temperature and velocity fields in the mould region using a strongly coupled flow model in which the effect of gap size and thermal contact resistance on heat transfer from the molten steel to the surrounding mould wall is taken into account.

2. DEVELOPMENT OF THE MODEL

2.1 Governing Field Equations

The field equations governing the heat transfer and fluid flow include the continuity equation, the Navier-Stokes equations and the energy equation, which can be expressed by

$$u_{i,i} = 0\,, \qquad (1)$$

$$\rho(\frac{\partial u_i}{\partial t} + u_j u_{i,j}) + p_{,i} - (\mu_{eff}(u_{i,j} + u_{j,i}))_{,j} = \rho g_i (1 - \beta(T - T_\beta)) - S_u\,, \qquad (2)$$

$$\rho c_p (\frac{\partial T}{\partial t} + u_j T_{,j}) = (\lambda_{eff} T_{,j})_{,j} - S_T\,. \qquad (3)$$

The flow inside the mushy(solidification) region is analogous to the flow through porous media. According to Darcy's law, which governs the flow of fluids through porous media, the source term S_u in equation (2) is proportional to the velocity of the liquid relative to the porous media and is given by (Reddy, 1992)

$$S_u = -(\mu / \kappa) u_r,$$

where κ denotes the permeability of steel defined by

$$\kappa = f(T)^3 / C(1 - f(T))^2$$

with the liquid fraction $f(T)$ given by

$$f(T) = \begin{cases} 1 & , T > T_L, \\ \dfrac{T - T_S}{T_L - T_S} & , T_S \le T \le T_L, \\ 0 & , T < T_S. \end{cases} \qquad (4)$$

The influence of turbulence on the transport of momentum and energy is modelled by the addition of the turbulent viscosity to the laminar viscosity and the turbulent conductivity to the molecular conductivity, yielding the effective viscosity μ_{eff} and the effective thermal conductivity λ_{eff} in equations 2 and 3 given by

$$\mu_{eff} = \mu + \mu_t, \quad \lambda_{eff} = \lambda + c_p \mu_t / \sigma_t,$$

where σ_t is the turbulent Prandtl number assumed as 0.9 (Thomas et al., 1994). Using the Prandtl-Kolmogorov law, the turbulent viscosity is determined by (Thomas et al., 1994)

$$\mu_t = \rho C_\mu k^2 / \varepsilon,$$

where k is the local turbulent energy, and ε is the rate of dissipation of turbulent energy. As the extended k-ε model due to Jaeger and Dhatt (1992) can be used for not only the turbulent region but also the near-wall region, we adopt this extended k-ε model and take into account the effect of temperature gradient. Thus, the k and ε fields can be determined by the following k-ε equations

$$\rho\left(\frac{\partial k}{\partial t} + u_j k_{,j}\right) - \left(\left(\mu + \frac{\mu_t}{\sigma_k}\right) k_{,j}\right)_{,j} = -\frac{\mu_t}{\sigma_t} \beta g_j T_{,j} + \mu_t G - \rho\varepsilon, \qquad (5)$$

$$\rho\left(\frac{\partial \varepsilon}{\partial t} + u_j \varepsilon_{,j}\right) - \left(\left(\mu + \frac{\mu_t}{\sigma_\varepsilon}\right) \varepsilon_{,j}\right)_{,j} = C_1 (1 - C_3) \frac{\varepsilon}{k} \frac{\mu_t}{\sigma_t} \beta g_j T_{,j} + C_1 C_{\varepsilon 1} \frac{\varepsilon}{k} \mu_t G - \rho C_2 C_{\varepsilon 2} \frac{\varepsilon^2}{k}, \qquad (6)$$

where

$$G = 2 \epsilon_{ij} \epsilon_{ij} \text{ with } \epsilon_{ij} = (u_{i,j} + u_{j,i})/2.$$

The values of the five empirical constants in equations (5) and (6), according to Launder and Spalding (1974), are taken to be C_1=1.44, C_2=1.92, C_3=0.80, σ_k=1.0 and σ_ε=1.3. For the solidification problem in the continuous casting of steel, C_μ is modified by (Shyy et al., 1992)

$$C_\mu = 0.09 f_\mu, \qquad (7)$$

where

$$f_\mu = \sqrt{f(T)} \exp(-3.4 / (1 + R_t / 50)^2)$$

represents the generalised damping mechanism of turbulent transport in both liquid and mushy regions, and R_t denotes the local turbulent Reynolds number defined by

$$R_t = \frac{\rho k^2}{\mu\varepsilon}. \qquad (8)$$

To ensure that none of the terms in equation (6) goes to infinity as k approaches zero, the low-Reynolds model of Launder-Sherma (Launder and Spalding, 1974) is adopted by choosing

$$C_{\varepsilon 1} = 1, \; C_{\varepsilon 2} = \begin{cases} 1 - 0.3\exp(-R_t^2), & k > 10^{-4}, \\ 1 - \exp(-R_t^2) & , otherwise. \end{cases} \qquad (9)$$

The heat source term S_T in equation (3) is set to zero everywhere except in the mushy region in which

$$S_T = \rho\left(\frac{\partial L f(T)}{\partial t} + u_j (L f(T))_{,j}\right), \qquad (10)$$

where L is the emitted latent heat when local freezing in the mushy zone occurs. Substituting S_T into equation (3), we have

$$\frac{\partial T}{\partial t} + u_j T_{,j} = (\alpha_{eff} T_{,j})_{,j}, \qquad (11)$$

where the effective diffusivity α_{eff} is determined by

$$\alpha_{eff} = \begin{cases} \dfrac{\lambda_{eff}}{\rho(c_p + L/(T_L - T_S))}, & T_S \le T \le T_L \\ \dfrac{\lambda_{eff}}{\rho c_p}, & otherwise. \end{cases} \quad (12)$$

2.2 Boundary Conditions

Consider a computation region shown in Figure 1.

- At the meniscus Γ_o

$$u=0, \; \frac{\partial T}{\partial n} = \frac{\partial k}{\partial n} = \frac{\partial \varepsilon}{\partial n} = 0 . \quad (13)$$

- At the nozzle inlet Γ_n

$$u= U_{in}, \; T=T_{in}. \quad (14)$$

- At the nozzle wall $\overline{\Gamma}_n$

$$u= 0, \; T=T_{in}. \quad (15)$$

- At the solidified steel strand Γ_w

$$u= U_{cast} . \quad (16)$$

- At the planes of symmetry Γ_{sym} and at the outflow boundary Γ_{exit}

$$u_x =0, \; \frac{\partial u}{\partial n} = \frac{\partial T}{\partial n} = \frac{\partial k}{\partial n} = \frac{\partial \varepsilon}{\partial n} = 0 , \quad (17)$$

where n is the unit vector normal to the boundary.

The heat flow across the lubrication layer to the surrounding mould has been shown by Hill and Wu (1994) to be

$$Q = h_\infty (T_w - T_\infty) = \frac{T_u - T_w}{R} = \frac{\lambda_g (T_{surf} - T_u)}{gap} = -\lambda \frac{\partial T_{surf}}{\partial n}, \quad (18)$$

from which we obtain

$$T_u = \frac{\gamma R T_{surf} + T_w}{1+\gamma R}, \quad T_w = \frac{\gamma T_{surf} + h_\infty (1+\gamma R) T_\infty}{h_\infty + \gamma R h_\infty + \gamma}, \quad (19)$$

where $\gamma = \lambda_g / gap$. The energy flux boundary condition at the solidified steel shell surface in the mould region can now be written as

$$-\lambda \frac{\partial T_{surf}}{\partial n} = h^*_\infty (T_{surf} - T_\infty) , \quad (20)$$

where

$$h^*_\infty = \gamma h_\infty / (h_\infty + \gamma R h_\infty + \gamma) .$$

If the temperature on the strand surface is greater than the solidified temperature of steel, condition (20) is replaced by(Wu et al, 1994)

$$-\lambda \frac{\partial T_{surf}}{\partial n} = h_\infty (T_{surf} - T_\infty) . \quad (21)$$

Below the mould, the heat flux from the strand surface to the environment may be defined as

$$-\lambda \frac{\partial T_{surf}}{\partial n} = h_\alpha (T_{surf} - T_\infty) + \omega\sigma (T^4_{surf} - T^4_{ext}), \quad (22)$$

where the first and the second terms on the right hand side represent heat transfer by conduction and radiation respectively.

Now we have a system of five equations (1-3 and 5-6) in terms of five unknown functions u, p, T, k and ε which describe the two dimensional coupled heat transfer - solidification - fluid flow problems occurring in the casting mould. Due to the symmetry of the flow problem, only a half of the casting region is considered.

3. PENALTY FINITE ELEMENT FORMULATION

Let $L^2(\Omega)$ be the space of functions that are square integrable over a bounded open set Ω of R^2 with boundary $\Gamma = \Gamma_0 \cup \Gamma_w \cup \Gamma_n \cup \overline{\Gamma}_n \cup \Gamma_{exit} \cup \Gamma_{sym}$ as shown in Figure 2. Thus, for any non-negative integer k,

$$H^k(\Omega) = \{q \in L^2(\Omega) : D^n q \in L^2(\Omega)\}, \; n=1,...,k$$

defines a Sobolev space, where D^n denotes all possible derivatives of order n. For vector

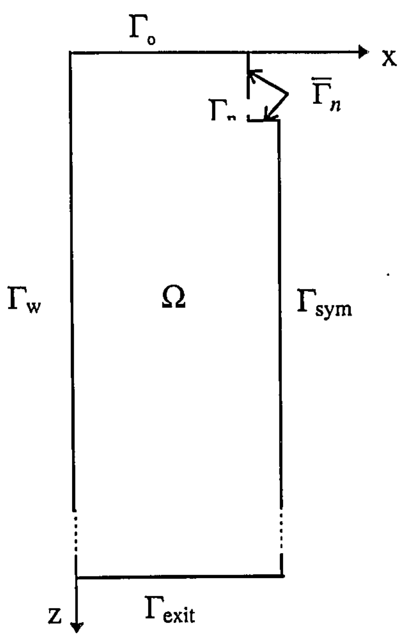

Fig 2. Computational domain with boundaries

valued functions, let $\mathbf{H}^k(\Omega)$ be the space of functions each of whose components belongs to $H^k(\Omega)$. To solve the coupled system constituted by equations (1-3) and (5-6) using the penalty method, the continuity requirement (1) is weakened and replaced by

$$u_{i,i} = -\delta \bar{p} \quad , \qquad (23)$$

where $\bar{p} = p - \rho g z$, and δ is a small positive number in the order of 10^{-4}-10^{-8}. Thus, the problem becomes to find u in $\mathbf{H}^1(\Omega)$ and $\bar{p}$, T, k and ε in $H^1(\Omega)$ satisfying equations (1-3) and (5-6) in the sense of weighted average. Following the usual finite element formulation, the following equations are eventually obtained

$$\begin{aligned} C^T U &= -\delta M_p \bar{p}^e, \\ M\dot{U} + AU + D_u U - \bar{C}\bar{p}^e &= F_u, \\ M\dot{T} + AT + D_T T + K_b T &= F_b, \qquad (24) \\ M\dot{K} + AK + D_k K &= F_k, \\ M\dot{E} + AE + D_\varepsilon E &= F_\varepsilon, \end{aligned}$$

where U, T, K and E are vectors representing the values of corresponding unknowns at the nodes of the element. Formulae for the calculation of coefficient matrices can be found from Wiwatanapataphee el al(1997).

From equation $(24)_1$, we have

$$\bar{p}^e = -(1/\delta) M_p^{-1} C^T U, \qquad (25)$$

which is then used to eliminate the pressure in the momentum equation, and thus the finite element equations for a typical element are

$$\begin{aligned} M\dot{U} + AU + D_U U + \frac{1}{\delta}\bar{C}M_p^{-1}C^T U &= F_U, \\ M\dot{T} + AT + D_T T + K_b T &= F_b, \qquad (26) \\ M\dot{K} + AK + D_k K &= F_k, \\ M\dot{E} + AE + D_\varepsilon E &= F_\varepsilon. \end{aligned}$$

By assembling the element equations over all elements, we obtain the following two systems of first order nonlinear ordinary differential equations

$$\begin{bmatrix} M & 0 \\ 0 & M \end{bmatrix}\begin{bmatrix} \dot{U} \\ \dot{T} \end{bmatrix} + \begin{bmatrix} A + D_u & 0 \\ 0 & A + D_T + K_b \end{bmatrix}\begin{bmatrix} U \\ T \end{bmatrix} + \begin{bmatrix} \frac{1}{\delta}\bar{C}M_p^{-1}C^T & 0 \\ 0 & 0 \end{bmatrix}\begin{bmatrix} U \\ T \end{bmatrix} = \begin{bmatrix} F_u \\ F_b \end{bmatrix}, \qquad (27)$$

$$\begin{bmatrix} M & 0 \\ 0 & M \end{bmatrix}\begin{bmatrix} \dot{K} \\ \dot{E} \end{bmatrix} + \begin{bmatrix} A + D_k & 0 \\ 0 & A + D_\varepsilon \end{bmatrix}\begin{bmatrix} K \\ E \end{bmatrix} = \begin{bmatrix} F_k \\ F_\varepsilon \end{bmatrix}, \qquad (28)$$

or in matrix form

$$M\dot{V} + [A + D + K_p]V = F, \qquad (29)$$

$$M^*\dot{V}^* + [A^* + D^*]V^* = F^*, \qquad (30)$$

where $V=(U_1,U_2,T)^T$ and $V^*=(K,E)^T$ are global vectors and all coefficient matrices refer to global matrices. Matrices M and M^* correspond to the transient term, matrices A and A^* correspond to the advection (convection) term, matrices D and D^* are due to the diffusion term, matrix K_p represents the penalty term, vector F provides forcing functions for the system and vector F^* represents the production dissipation. We note that matrices M and M^* are symmetric by construction.

4. METHOD OF SOLUTION

A system of nonlinear ordinary differential equations can be solved by using either an implicit or an explicit time integration scheme. Here, we present a simple explicit time integration scheme to solve equations (29) and (30) based on the forward Euler method. The algorithm is as follows

Step 1. Set up initial conditions

- Set the velocity to zero and temperature to pouring temperature at all nodes
- Find laminar solution $\{u_1^0, u_2^0, T^0\}$ by solving equation (29)
- Set the turbulent energy and the rate of dissipation of turbulent energy to small positive values $\{k^0, \varepsilon^0\}$
- Set the production-dissipation terms F^* to zero

Step 2. Solve k-ε equations at t^{n+1}

- Update coefficient matrices A^*, D^* and production -dissipation vector F^*
- Apply boundary conditions to the system of equations (30)
- Update the solution at time step Δt by

$$V^{*n+1} = V^{*n} + \Delta t M^{*-1}[F^{*n} - A^{*n}V^{*n} - D^{*n}V^{*n}] \qquad (31)$$

Step 3. Solve the coupled NS-Energy equations

- Update eddy viscosity
- Update coefficient matrices A, D, K_p and vector F
- Apply boundary conditions to the system of equations (29)
- Update the solution at time step Δt by

$$V^{n+1} = V^n + \Delta t M^{-1}[F^n - (A^n + D^n + K_p)V^n] \quad (32)$$

Step 4. Repeat step 2 and 3 until the sequence $\{V^{n+1}, V^{*n+1}\}$ converges to a steady state solution.

A computer program has been developed for the solution of the present problem. In the development of this program, the reduced storage mode is used for matrices A, D, A^*, D^* and K_p where only the elements between the leftmost and the rightmost nonzero elements in each row, are stored into one dimensional arrays. The matrices M and M^* are lumped into diagonal matrices.

5. NUMERICAL EXAMPLE

In this example, we study the heat transfer and fluid flow in a mould of depth 0.75 metre and half-width 0.875 metre. The position of the nozzle inlet is shown in Figure 3. The solution is limited to a depth of 8 metres below the meniscus. With the computer resources available and a mesh-sensitivity study, the finite element mesh constructed for the present study consists of 687 elements and 751 nodes. Based on the above algorithm with $\Delta t = 10^{-4}$, over 20,000 time-steps are required to achieve a converged solution. This takes approximately 8 CPU hours on a Silicon Graphics 4D/35 workstation.

Table 1. Numerical data

Pouring temperature T_{in}(°C)	1530
Reference temperature T_β(°C)	1497.5
Molten temperature T_L(°C)	1525
Solidified temperature T_S(°C)	1465
Temperature of cooling water T_∞ (°C)	20
External temperature T_{ext}(°C)	100
Pouring velocity U_{in}(m/s)	(-1.0456,0.280)
Casting velocity U_{cast}(m/s)	(0.0,0.02167)
Gravitational acceleration g(m/s^2)	9.8
Density of steel ρ(kg/m^3)	7800
Viscosity of steel μ(Pa.s)	0.001
Specific heat c_p(J/kg °C)	465
Thermal conductivity of steel λ(W/m °C)	35
Thermal conductivity of flux λ_g(W/m °C)	1.0
Latent heat L(J/kg)	2.72x10^5
Heat transfer coefficient h_∞ (W/m^2 °C	10^4
Thermal expansion of steel β(°C^{-1})	0.00003
Emissivity of solid steel ω	0.4
Stefan-Bolzmann constant σ (W/m^2 K^4)	5.66x10^{-8}
Thickness of flux layer gap(m)	10^{-3},10^{-4}
Thermal contact resistance R(m^2 °C/W)	10^{-4},10^{-5}
Morphology constant C (/m^2)	1.8x10^6
Penalty number δ	10^{-4}

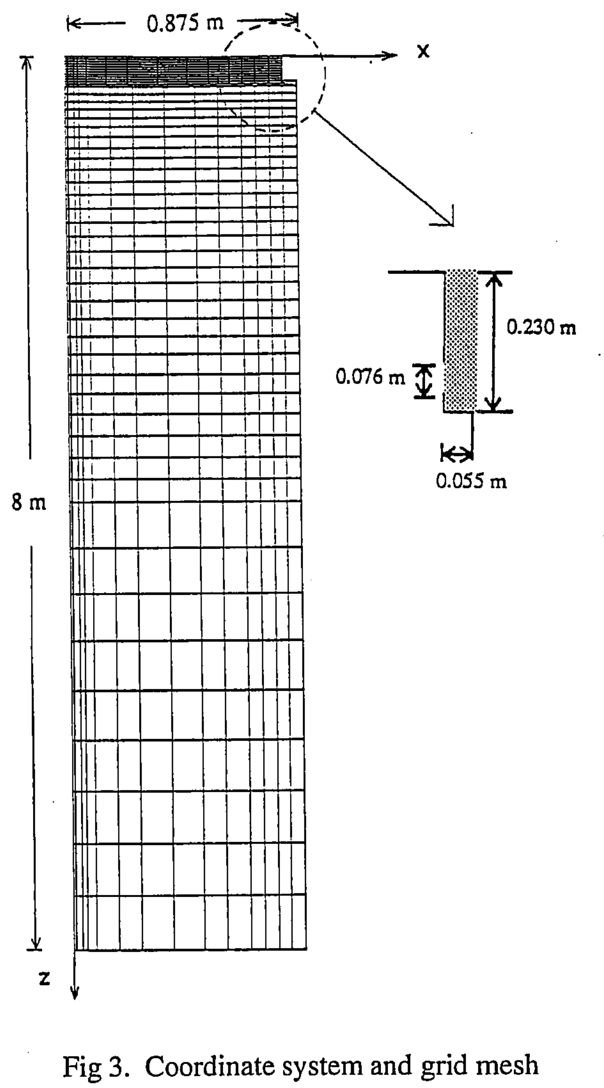

Fig 3. Coordinate system and grid mesh

Using the numerical data in Table 1, the features of fluid flow and heat transfer below the meniscus are shown in Figures 4 and 5, respectively. The flow pattern shows that there exist three circulating zones in the top part of the casting. The flow becomes parallel further downstream. Two sets of gap size and thermal contact resistance between the mould wall and the steel strand have been used in computations to investigate their impact on the resulting solidification characteristics. The computed temperature profiles and the thickness of solidified steel shells for different values of thermal contact resistance and gap size are compared in Figures 5(a) and 5(b). These results show that changes in thickness of the lubrication gap and thermal contact resistance affect the thickness of the solidified steel shell. Distributions of turbulence quantities k and ε are shown in Figure 6 and 7. The quantities of k and ε are very high near the nozzle opening. They rapidly decrease in the circulating region and then reach the smallest level in the solidified steel shell and below the mould region. These results indicate that the appearance of highly turbulent flow is in the upper region of the casting mould.

6. CONCLUSION

A two-dimensional penalty finite element model has been developed to study the strongly coupled heat transfer - solidification - fluid flow in the continuous steel casting process. The study shows that the modified k-ε model can produce a velocity profile which changes smoothly in the mould region. Recirculations of molten steel are found to occur in the mould region. Furthermore, the thickness of the solidified steel shell at the bottom of the mould varies with the change of gap size and thermal contact resistance. It increases with a decrease of the thermal contact resistance and gap size.

REFERENCES

Choudhary, S.K and Mazumdar, D., 1994, "Mathematical modelling of transport phenomena in continuous casting of steel", *ISIJ International*, 34(7), pp.584-592.

Flint, P.J., 1990, "A three-dimensional finite difference model of heat transfer, fluid flow and solidification in the continuous slab caster", *Steelmaking Conference Proceedings*, pp.481- 490.

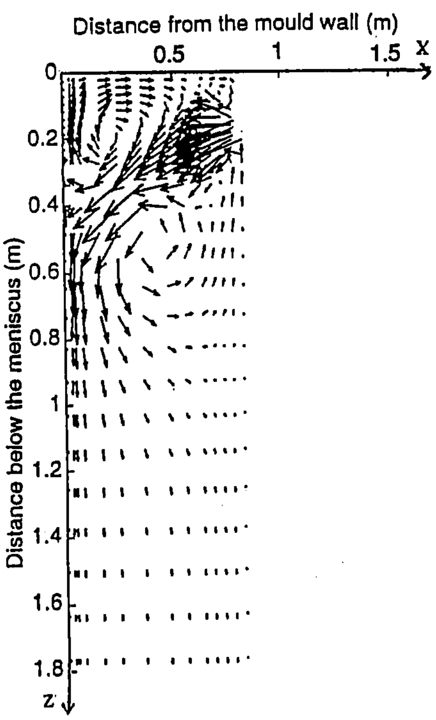

Fig 4. Velocity field (m/s)

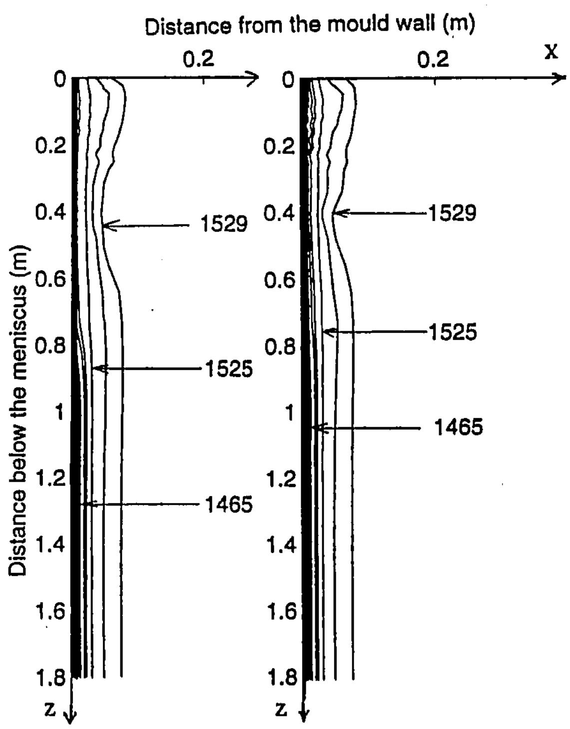

Fig 5. Temperature distribution (°C)
(a) R=10^{-4} m^2 °C/W, gap=10^{-3} m
(b) R=10^{-5} m^2 °C/W, gap=10^{-4} m

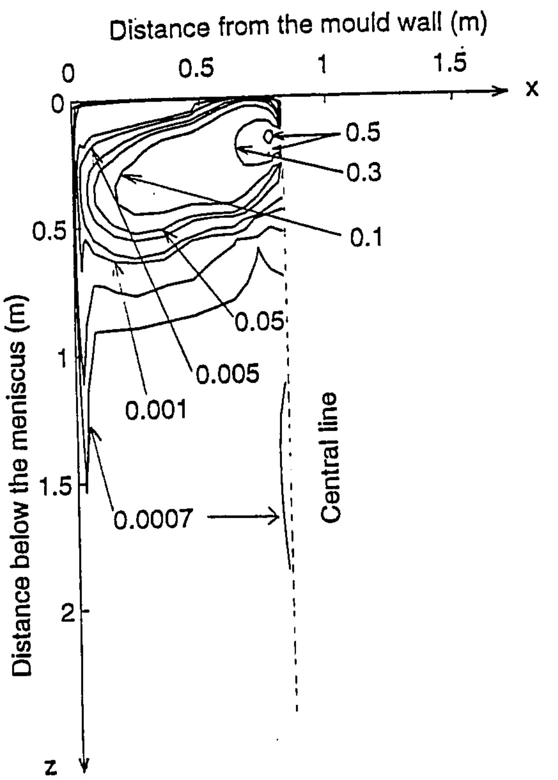

Fig 6. Contour plot of turbulent kinetic energy (m^2/s^2)

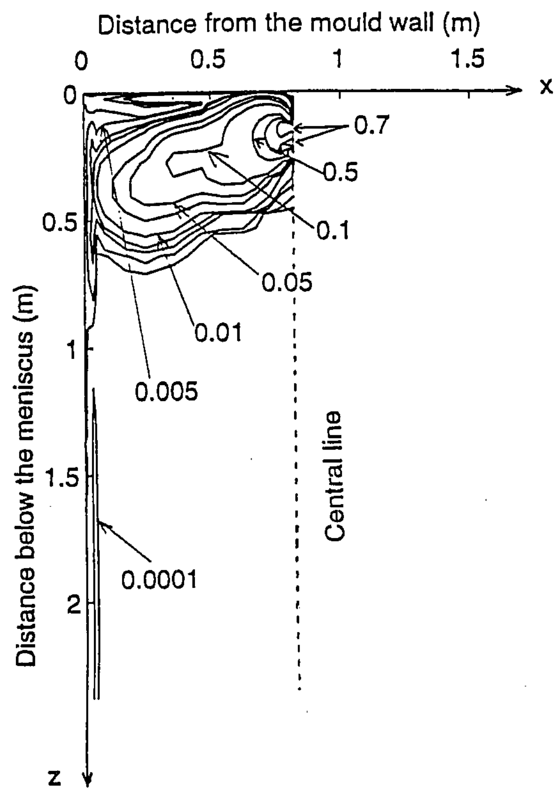

Fig 7. Contour plot of dissipation rate (m^2/s^3)

Hill, J.M., Wu, Y-H. and Wiwatanapataphee, B., 1997, "Analysis of flux flow and the formulation of oscillation marks in the continuous caster", submitted to *Journal of Engineering Mathematics*.

Hill,J.M. and Wu,Y-H., 1994, "On a nonlinear Stefan problem arising in the continuous casting of steel", *Acta Mechanica*, 107, pp. 183-198.

Jaeger, M. and Dhatt, G., 1992, "An extended *k-ε* finite element model", *International Journal of Numerical Methods in Fluids*, 14, pp.1325-1345.

Launder, B.E. and Spalding, D.B., 1974, "The numerical computation of turbulent flows", *Computer Methods in Applied Mechanics and Engineering* 3, pp.269-289.

Reddy, M.P. and Reddy, J.N., 1992, "Numerical simulation of forming processes using a coupled fluid flow and heat transfer model", *International Journal for Numerical Methods for Engineering*, 35, pp.807-833.

Shyy, W., Pang, Y., Hunter, G.B., Wei, D.Y. and Chen, M.-H., 1992, "Modelling of turbulent transport and solidification during continuous ingot casting", *International Journal of Heat Mass Transfer*, 35(5), pp.1229-1245.

Thomas, B.G., Huang,X. and Sussman, R.C., 1994, "Simulation of argon gas flow effects in continuous slab caster", *Metallurgical and Materials Transactions B*, 25B, pp.527-547.

Wiwatanapataphee B., Wu, Y-H. and Siew, P.F., 1997, Report, School of Mathematics and Statistics, Curtin University of Technology, WA.

Wu, Y-H., Hill, J.M. and Flint, P.J., 1994, "A novel finite element method for heat transfer in the continuous caster", *J.Austral.Math.Soc. Ser.B*, 35, pp. 263-288.